

1  
2  
3  
4  
5  
6  
7  
8  
9  
10  
11  
12  
13  
14  
15  
16  
17  
18  
19  
20  
21  
22  
23  
24  
25  
26  
27  
28

## **Revision 2**

### **Lavinskyite, $K(\text{LiCu})\text{Cu}_6(\text{Si}_4\text{O}_{11})_2(\text{OH})_4$ , isotypic with planchéite, a new mineral from the Wessels mine, Kalahari Manganese Fields, South Africa**

Hexiong Yang<sup>1</sup>, Robert T. Downs<sup>1</sup>, Stanley H. Evans<sup>1</sup>, and William W. Pinch<sup>2</sup>

<sup>1</sup>Department of Geosciences, University of Arizona, Tucson, Arizona 85721-0077, U.S.A.

<sup>2</sup>19 Stonebridge Lane, Pittsford, New York 14534, U.S.A.

Corresponding author: [hyang@u.arizona.edu](mailto:hyang@u.arizona.edu)

#### **Abstract**

A new mineral species, lavinskyite, ideally  $K(\text{LiCu}^{2+})\text{Cu}_6^{2+}(\text{Si}_4\text{O}_{11})_2(\text{OH})_4$  (IMA 2012-028), has been found in the Wessels mine, Kalahari Manganese Fields, Northern Cape Province, South Africa. Associated minerals include wesselsite, pectolite, richterite, sugilite, and scottyite. Lavinskyite crystals are tabular [parallel to (010)]. The mineral is light blue, transparent with very pale blue streak and vitreous luster. It is brittle and has a Mohs hardness of ~5; cleavage is perfect on {010} and no parting was observed. The measured and calculated densities are 3.61(3) and 3.62 g/cm<sup>3</sup>, respectively. Optically, lavinskyite is biaxial (+), with  $\alpha = 1.675(1)$ ,  $\beta = 1.686(1)$ ,  $\gamma = 1.715(1)$ ,  $2V_{\text{meas}} = 64(2)^\circ$ . An electron microprobe analysis produced an average composition (wt.%) of SiO<sub>2</sub> 42.85(10), CuO 46.13(23), K<sub>2</sub>O 4.16(2), MgO 1.53(17), Na<sub>2</sub>O 0.27(4), BaO 0.18(6), and MnO 0.08(1), plus Li<sub>2</sub>O 1.38 from the LA-ICP-MS measurement and H<sub>2</sub>O 3.22 (added to bring the analytical total close to 100%), yielding a total of 99.79 % and an empirical chemical formula

$(\text{K}_{0.99}\text{Ba}_{0.01})_{\Sigma=1.00}(\text{Li}_{1.04}\text{Cu}_{0.93}\text{Na}_{0.10})_{\Sigma=2.07}(\text{Cu}_{5.57}\text{Mg}_{0.43}\text{Mn}_{0.01})_{\Sigma=6.01}(\text{Si}_{4.00}\text{O}_{11})_2(\text{OH})_4$ .

Lavinskyite is isotypic with planchéite,  $\text{Cu}_8(\text{Si}_4\text{O}_{11})_2(\text{OH})_4 \cdot \text{H}_2\text{O}$ , an amphibole derivative. It is orthorhombic, with space group *Pcnb* and unit-cell parameters  $a =$

29 19.046(2),  $b = 20.377(2)$ ,  $c = 5.2497(6)$  Å, and  $V = 2037.4(4)$  Å<sup>3</sup>. The key difference  
30 between lavinskyite and planchéite lies in the coupled substitution of K<sup>+</sup> and Li<sup>+</sup> in the  
31 former for H<sub>2</sub>O and Cu<sup>2+</sup> in the latter, respectively. The structure of lavinskyite is  
32 characterized by the undulating, brucite-like layers consisting of three distinct octahedral  
33 sites occupied mainly by Cu. These layers are sandwiched by the amphibole-type double  
34 silicate chains extending along the  $c$  axis, forming a sheet structure of compact silicate-  
35 Cu-silicate triple layers. Adjacent sheets are linked together by K and M4 (= Cu + Li)  
36 cations, as well as hydrogen bonding. The M4 site is split, with Cu and Li occupying two  
37 different sites. Lavinskyite exhibits more amphibole-like structural features than  
38 planchéite, as a consequence of K in the large cavity between the two back-to-back  
39 double silicate chains.

40

41 **Key words:** lavinskyite, K(LiCu)Cu<sub>6</sub>(Si<sub>4</sub>O<sub>11</sub>)<sub>2</sub>(OH)<sub>4</sub>, planchéite, crystal structure, X-ray  
42 diffraction, Raman spectra

43

44

45

## Introduction

46 A new mineral species, lavinskyite, ideally K(LiCu)Cu<sub>6</sub>(Si<sub>4</sub>O<sub>11</sub>)<sub>2</sub>(OH)<sub>4</sub>, has been  
47 found in the Wessels mine, Kalahari Manganese Fields, Northern Cape Province,  
48 Republic of South Africa. It is named in honor of Dr. Robert Matthew Lavinsky (born in  
49 1973), the founder and manager of Arkenstone, a sole proprietorship for dealing in  
50 collectible mineral specimens and crystals. The Arkenstone website ([www.iRocks.com](http://www.iRocks.com))  
51 was one of the first to bring mineral specimens to sale over the Internet. Dr. Lavinsky has  
52 been a donor of important mineral specimens to the Smithsonian Institution, Harvard  
53 University, California Institute of Technology, University of Arizona, and other  
54 institutions. He is also the largest contributor of information and photography to Mindat  
55 (an online public-access database of mineralogical information) and the sponsor of the

56 Tucson Mineral and Gem Show Juniors' Award. Dr. Lavinsky recognized that some  
57 mineral specimens he brought to the USA from South Africa appeared to represent new  
58 mineral species and provided samples to our laboratory. The new mineral and its name  
59 have been approved by the Commission on New Minerals, Nomenclature and  
60 Classification (CNMNC) of the International Mineralogical Association (IMA 2012-  
61 028). Part of the cotype sample has been deposited at the University of Arizona Mineral  
62 Museum (Catalogue # 19335) and the RRUFF Project (deposition # R120057). The  
63 holotype sample is in the collection of W.W. Pinch.

64 Lavinskyite is a Cu-bearing silicate with amphibole-type double chains. Cu-  
65 bearing chain silicates are relatively rare in nature. In addition to lavinskyite, planchéite  
66  $\text{Cu}_8(\text{Si}_4\text{O}_{11})_2(\text{OH})_4 \cdot \text{H}_2\text{O}$  (Evans and Mrose 1977), shattuckite  $\text{Cu}_5(\text{Si}_2\text{O}_6)_2(\text{OH})_2$  (Evans  
67 and Mrose 1966, 1976; Kawahawa 1977) and liebauite  $\text{Ca}_6\text{Cu}_{10}(\text{Si}_{18}\text{O}_{52})$  (Zöller et al.  
68 1992) also belong to this group. Nonetheless, there have been a number of reports on  
69 synthetic Cu-bearing chain silicates, such as  $\text{Na}_2\text{Cu}_3(\text{Si}_4\text{O}_{12})$  (Kawamura and Kawahara  
70 1976),  $\text{Na}_4\text{Cu}_2(\text{Si}_8\text{O}_{20})$  (Kawamura and Kawahara 1977),  $\text{CuMg}(\text{Si}_2\text{O}_6)$  (Breuer et al.  
71 1986),  $\text{CaBa}_3\text{Cu}(\text{Si}_6\text{O}_{17})$  (Angel et al. 1990), and  $\text{Li}_2(\text{Mg,Cu})\text{Cu}_2(\text{Si}_2\text{O}_6)_2$  (Horiuchi et al.  
72 1997). Moreover, Kawamura et al. (1976) successfully synthesized planchéite under  
73 hydrothermal conditions at 350-500 °C and 1-2 kbars. This paper describes the physical  
74 and chemical properties of lavinskyite and its structure determination using single-crystal  
75 X-ray diffraction.

76  
77

## 78 **Sample Description and Experimental Methods**

### 79 *Occurrence, physical and chemical properties, and Raman spectra*

80 Lavinskyite was found on two specimens originating from the central-eastern ore  
81 body of the Wessels mine, Kalahari Manganese Fields, Northern Cape Province,  
82 Republic of South Africa. It is in a massive assemblage associated with wesselsite

83 SrCuSi<sub>4</sub>O<sub>10</sub>, scottyite BaCu<sub>2</sub>Si<sub>2</sub>O<sub>7</sub>, pectolite NaCa<sub>2</sub>Si<sub>3</sub>O<sub>8</sub>(OH), richterite  
84 Na(CaNa)Mg<sub>5</sub>Si<sub>8</sub>O<sub>22</sub>(OH)<sub>2</sub>, and sugilite KNa<sub>2</sub>Fe<sup>3+</sup><sub>2</sub>(Li<sub>3</sub>Si<sub>12</sub>)O<sub>30</sub> (Figs. 1 and 2). The  
85 mineral assemblage probably formed as a result of a hydrothermal event. Conditions  
86 during metamorphism were in the range of 270-420 °C at 0.2-1.0 kbar (Kleyenstuber  
87 1984; Gutzmer and Beukes 1996). Detailed reviews of the geology and mineralogy of the  
88 Kalahari Manganese Fields have been given by Kleyenstuber (1984), Von Bezing et al.  
89 (1991), and Gutzmer and Beukes (1996).

90 Lavinskyite crystals are tabular [parallel to (010)]; broken pieces are usually  
91 bladed, elongated along [001], up to 0.5 × 0.3 × 0.1 mm. No twinning is observed. The  
92 mineral is light blue, transparent with very pale blue streak and vitreous luster. It is brittle  
93 and has a Mohs hardness of ~5; cleavage is perfect on {010} and no parting is observed.  
94 The measured and calculated densities are 3.61(3) and 3.62 g/cm<sup>3</sup>, respectively.  
95 Optically, lavinskyite is biaxial (+), with  $\alpha = 1.675(1)$ ,  $\beta = 1.686(1)$ ,  $\gamma = 1.715(1)$  (white  
96 light),  $2V$  (meas.) = 64(2)°,  $2V$  (calc.) = 64.2°, and the orientation  $X = a$ ,  $Y = b$ ,  $Z = c$ .  
97 The pleochroism is  $X = \text{dark blue}$ ,  $Y = \text{light blue}$ , and  $Z = \text{light blue}$ , and the absorption  $X$   
98  $> Y = Z$ . No dispersion was observed. Lavinskyite is insoluble in water, acetone, or  
99 hydrochloric acid.

100 The chemical composition of lavinskyite was determined using a CAMECA SX-  
101 100 electron microprobe (15 kV, 20 nA, < 1 μm beam diameter). The standards included  
102 chalcopyrite (Cu), NBS\_K458 (Ba), diopside (Si, Mg), rhodonite (Mn), orthoclase (K),  
103 and albite (Na), yielding an average composition (wt.%) (8 points) of SiO<sub>2</sub> 42.85(10),  
104 CuO 46.13(23), K<sub>2</sub>O 4.16(2), MgO 1.53(17), Na<sub>2</sub>O 0.27(4), BaO 0.18(6), and MnO  
105 0.08(1), and total = 95.19(26). The content of Li<sub>2</sub>O (1.38 wt.%) was measured with a LA-  
106 ICP-MS mass spectrometer. The H<sub>2</sub>O content (3.22 wt.%) was added to bring the  
107 analytical total close to 100%. The resultant chemical formula, calculated on the basis of  
108 26 O *apfu* (from the structure determination), is

109  $(\text{K}_{0.99}\text{Ba}_{0.01})_{\Sigma=1.00}(\text{Li}_{1.04}\text{Cu}_{0.93}\text{Na}_{0.10})_{\Sigma=2.07}(\text{Cu}_{5.57}\text{Mg}_{0.43}\text{Mn}_{0.01})_{\Sigma=6.01}(\text{Si}_{4.00}\text{O}_{11})_2(\text{OH})_4$ , which can be  
110 simplified to  $\text{K}(\text{LiCu}^{2+})\text{Cu}^{2+}_6(\text{Si}_4\text{O}_{11})_2(\text{OH})_4$ .

111 The Raman spectrum of lavinskyite was collected from a randomly oriented  
112 crystal on a Thermo Almega microRaman system, using a 532-nm solid-state laser with a  
113 thermoelectric cooled CCD detector. The laser is partially polarized with  $4\text{ cm}^{-1}$   
114 resolution and a spot size of  $1\ \mu\text{m}$ .

115

#### 116 *X-ray crystallography*

117 The powder X-ray diffraction data of lavinskyite were collected on a Bruker D8  
118 Advance diffractometer with  $\text{Cu } K_{\alpha}$  radiation. Listed in Table 1 are the experimental  $d$ -  
119 spacing and relative intensity data for observed strong peaks, along with the  
120 corresponding values calculated from the determined structure using the program XPOW  
121 (Downs et al. 1993). Single-crystal X-ray diffraction data of lavinskyite were collected on  
122 a Bruker X8 APEX2 CCD X-ray diffractometer equipped with graphite-  
123 monochromatized  $\text{Mo } K_{\alpha}$  radiation, with frame widths of  $0.5^{\circ}$  in  $\omega$  and 30 s counting  
124 time per frame. All reflections were indexed on the basis of an orthorhombic unit-cell  
125 (Table 2). The intensity data were corrected for X-ray absorption using the Bruker  
126 program SADABS. The systematic absences of reflections suggest the unique space  
127 group *Pcnb* (#60). The crystal structure was solved and refined using SHELX97  
128 (Sheldrick 2008).

129 During the structure refinements, for simplicity, the small amounts of Na, Ba, and  
130 Mn, detected from the electron microprobe analysis, were ignored. A preliminary  
131 refinement indicated that the M2 and M3 sites are filled with Cu only, whereas the M1  
132 and M4 sites show the mixed occupations by (Cu + Mg) and (Cu + Li), respectively. The  
133 A site is fully occupied by K. Furthermore, the M4 site appears to be split, with the M4a  
134 and M4b sites separated by about  $0.9\ \text{\AA}$ . Thereby, the following assignments of atoms  
135 into different sites were made in the subsequent refinements: A = K, M1 =  $(0.775\text{Cu} +$

136 0.225Mg), M2 = Cu, M3 = Cu, M4a = (0.5Li + ), and M4b = (0.5Cu + ), giving rise to  
137 the structure formula  ${}^A\text{K}^{\text{M4}}(\text{LiCu})^{\text{M1}}(\text{Cu}_{1.57}\text{Mg}_{0.43})^{\text{M2M3}}\text{Cu}_4(\text{Si}_4\text{O}_{11})_2(\text{OH})_4$ . The positions  
138 of all atoms were refined with anisotropic displacement parameters, except for H and Li  
139 atoms, the former being refined with a fixed  $U_{\text{iso}}$  parameter (= 0.04) and the latter with  
140  $U_{\text{iso}}$  varied. Final coordinates and displacement parameters of atoms in lavinskyite are  
141 listed in Table 3, and selected bond-distances in Table 4.

142

143

## Discussion

144 *Crystal structure*

145 Lavinskyite is isotypic with planchéite, demonstrated to be an amphibole  
146 derivative by Evans and Mrose (1977). Table 5 compares some mineralogical data for the  
147 two minerals. The key difference between lavinskyite and planchéite lies in the coupled  
148 chemical substitution of  $\text{K}^+$  and  $\text{Li}^+$  in the former for  $\text{H}_2\text{O}$  and  $\text{Cu}^{2+}$  in the latter,  
149 respectively. The crystal structure of lavinskyite is characterized by the undulating,  
150 brucite-like layers consisting of M1, M2, and M3 octahedra. These layers are parallel to  
151 (010) and are sandwiched by the amphibole-type double silicate chains extending along  
152 the *c* axis, forming a sheet structure in terms of the compact silicate-Cu-silicate triple  
153 layers (Figs. 3 and 4). Adjacent sheets are linked together by the A and M4 cations.  
154 Interestingly, our structure refinement shows that Cu and Li at the M4 site are split,  
155 occupying different M4a and M4b sites, respectively. The compact silicate-Cu-silicate  
156 triple layer in lavinskyite explains its perfect {010} cleavage and elongation along [001].

157 Each double silicate chain in lavinskyite is composed of four unique  $\text{SiO}_4$   
158 tetrahedra (Si1, Si2, Si3, and Si4), with Si1 and Si2 forming the single silicate A chain  
159 and Si3 and Si4 the B chain (Fig. 3). Thus far, such a conformation of double silicate  
160 chains has only been observed in monoclinic  $P2_1/a$  amphibole (joesmithite) (Moore et al.  
161 1993). In comparison, each double silicate chain in most common  $C2/m$ ,  $P2_1/m$ , and  
162  $Pnma$  amphiboles comprises only two unique  $\text{SiO}_4$  tetrahedra. The kinking angle, defined

163 by the bridging oxygen atoms, of the B chain ( $\angle\text{O9-O10-O9} = 172.5^\circ$ ) is greater than that  
164 of the A chain ( $\angle\text{O6-O7-O6} = 168.3^\circ$ ). Moreover, the two  $\text{SiO}_4$  tetrahedra in the B chain  
165 are both more distorted than those in the A chain, as measured by the tetrahedral angle  
166 variance (TAV) and quadratic elongation (TQE) (Robinson et al. 1971) (Table 4).

167 Among four symmetrically non-equivalent Cu-dominant sites, the octahedrally-  
168 coordinated M1, M2, and M3 sites in the brucite-like layers are all distorted, with two M-  
169 O bonds noticeably longer than the other four bonds (Table 4). The M4a site, however, is  
170 in a nearly square-planar coordination. In contrast, the M4b site, partially occupied by Li,  
171 is in a markedly distorted octahedral coordination, with the Li-O bond distances ranging  
172 from 1.907(2) to 2.699(2) Å. The A site, occupied by  $\text{K}^+$ , is situated in a large cavity  
173 between the back-to-back double tetrahedral chains (Fig. 3), resembling that in  
174 amphiboles containing the A-type cations. The A site in planchéite is occupied by  $\text{H}_2\text{O}$   
175 (Evans and Mrose 1977).

176 There are two OH groups in the lavinskyite structure, O12-H1 and O13-H2. The  
177 H1 and H2 atoms are 0.76 and 0.74 Å away from OH12 and OH13, respectively. The  
178 bonding environment of the O12-H1 group is quite analogous to that of the OH groups in  
179 amphiboles, with two O12-H1 bonds pointing nearly to the A site from opposite  
180 directions ( $\angle\text{H1-A-H1} = 169.4^\circ$ ) (Fig. 4). The nearest O atom (O8) to O12 is 3.37 Å  
181 away, indicating that O12-H forms little or no hydrogen bonding with other O atoms. In  
182 contrast, the O13-H2 group forms a relatively strong hydrogen bond with O5 ( $\text{O13-O5} =$   
183  $2.91 \text{ Å}$ ,  $\angle\text{O13-H2}\dots\text{O5} = 170.7^\circ$ ). However, this hydrogen bond is only found on one  
184 side of the M4 site, not on the opposite (Fig. 4). Such an unbalanced distribution of the  
185 hydrogen bond around the M4 site may account in part for the corrugation of the brucite-  
186 like octahedral layers. The hydrogen bonds are reported to be responsible for the  
187 corrugation of the  $\text{CoO}_4(\text{H}_2\text{O})_2$  octahedral layers in the synthetic compound  
188  $\text{Co}_{2.39}\text{Cu}_{0.61}(\text{PO}_4)_2\cdot\text{H}_2\text{O}$  (Assani et al. 2010), as well as the Ca-polyhedral layers in  
189 vladimirite  $\text{Ca}_4(\text{AsO}_3\text{OH})(\text{AsO}_4)_2\cdot 4\text{H}_2\text{O}$  (Yang et al. 2011).

190

191 *Raman spectra*

192           The Raman spectrum of lavinskyite is displayed in Figure 5. Based on previous  
193 Raman spectroscopic studies on planchéite (Frost and Xi 2012) and various amphiboles  
194 (Rinaudo et al. 2004; Makreshi et al. 2006; Apopei and Buzgar 2010, and references  
195 therein), we made a tentative assignment of major Raman bands for lavinskyite (Table 6).  
196 As expected, the Raman spectrum of lavinskyite shows some features similar to those for  
197 both amphiboles and planchéite, especially in the O-H stretching region. Specifically,  
198 whereas all O-H stretching bands (at least five obvious ones) in planchéite are between  
199 2800 and 3500  $\text{cm}^{-1}$  (Frost and Xi 2012), those (1 to 4 obvious ones, depending on  
200 chemical compositions) in hydroxyl amphiboles (Rinaudo et al. 2004; Makreshi et al.  
201 2006) generally fall between 3600 and 3700  $\text{cm}^{-1}$ . For lavinskyite, we observe three  
202 apparent, sharp O-H stretching bands between 3600 and 3700  $\text{cm}^{-1}$ , as those in  
203 amphiboles, and a relatively weak and broad band (with a shoulder) at 3390  $\text{cm}^{-1}$ .  
204 Consequently, we attribute the three O-H stretching bands between 3600 and 3700  $\text{cm}^{-1}$   
205 to the vibrations of the amphibole-like O12-H1 group and the band at 3390  $\text{cm}^{-1}$  to the  
206 OH13-H2 vibration. According to the correlation between O-H stretching frequencies  
207 and O-H...O hydrogen bond lengths in minerals (Libowitzky 1999), the O-H stretching  
208 band at 3390  $\text{cm}^{-1}$  would correspond to an O-H...O distance of  $\sim 2.90$  Å, in accordance  
209 with the value from our structural determination. For planchéite, the presence of the  
210 multiple O-H stretching bands between 2800 and 3500  $\text{cm}^{-1}$  and the lack of the  
211 amphibole-like bands above 3600  $\text{cm}^{-1}$  are apparently due to the existence of H<sub>2</sub>O in the  
212 A site and may suggest that all H atoms are likely engaged in hydrogen bonding.

213           The discovery of lavinskyite adds a new member to the amphibole derivative  
214 group, and it evidently exhibits more amphibole-like structural features than planchéite,  
215 due to the presence of K in its large cavity between the two back-to-back double silicate  
216 chains. Furthermore, the crystal-chemical relationship between lavinskyite and planchéite



217 begs the question whether the amphibole structure can incorporate H<sub>2</sub>O in its A site as  
218 well, with the composition <sup>A</sup>(H<sub>2</sub>O)M<sub>7</sub>Si<sub>8</sub>O<sub>22</sub>(OH)<sub>2</sub>, where M represents divalent cations  
219 found in amphiboles. From the crystal structure point of view, there seems no obstacle for  
220 H<sub>2</sub>O to enter the A site in the amphibole structure, given its strong resemblance to that in  
221 planchéite. Based on the Raman spectroscopic measurement by Frost and Xi (2012), it  
222 appears that the occupation of H<sub>2</sub>O in the A site in planchéite result in the formation of  
223 multiple hydrogen bonds, as indicated by several obvious Raman bands between 2800  
224 and 3500 cm<sup>-1</sup>. The three shortest distances between O<sub>water</sub> in the A site and nearest  
225 O<sub>bridging</sub> are 2.62, 2.99, and 3.04 Å in planchéite (Evans and Mrose 1977). Accordingly,  
226 similar Raman spectral features in the OH stretching vibration region can be expected for  
227 H<sub>2</sub>O-bearing amphiboles if they could be found in nature or synthesized eventually.

228

229

### Acknowledgements

230 This study was funded by the Science Foundation Arizona.

231

232

233

### References Cited

234

235 Angel, B.J., Ross, N.L., Finger, L.W, and Hazen, R.M. (1990) Ba<sub>3</sub>CaCuSi<sub>6</sub>O<sub>17</sub>: A new  
236 {1B, I} [<sup>4</sup>Si<sub>6</sub>O<sub>17</sub>] chain silicate. *Acta Crystallographica*, C46, 2028-2030.

237 Apopei, A.I. and Buzgar, N. (2010) The Raman study of amphiboles. *Cuza Iasi Geologie*,  
238 56, 57-83.

239 Assani, A., Saadi, M., and EL Ammari, L. (2010) Dicobalt copper  
240 bis[orthophosphate(V)] monohydrate, Co<sub>2.39</sub>Cu<sub>0.61</sub>(PO<sub>4</sub>)<sub>2</sub>·H<sub>2</sub>O. *Acta*  
241 *Crystallographica*, E66, i44.

242 Breuer, K.-H., Eysel, W, and Behruzi, M. (1986) Copper(II) silicates and germanates  
243 with chain structures: II. Crystal chemistry. *Zeitschrift für Kristallographie*, 176,

- 244 219-232.
- 245 Downs, R.T., Bartelmehs, K.L., Gibbs, G.V. and Boisen, M.B., Jr. (1993) Interactive  
246 software for calculating and displaying X-ray or neutron powder diffractometer  
247 patterns of crystalline materials. *American Mineralogist*, 78, 1104-1107.
- 248 Evans, H.T., Jr., and Mrose, M.E. (1966) Shattuckite and planchéite: A crystal chemical  
249 study. *Science*, 154, 506-507.
- 250 Evans, H.T. and Mrose, M.E. (1977) The crystal chemistry of the hydrous copper  
251 silicates, shattuckite and planchéite. *American Mineralogist*, 62, 491-502.
- 252 Frost, R.L. and Xi, Y. (2012) A vibrational spectroscopic study of planchéite  
253  $\text{Cu}_8\text{Si}_8\text{O}_{22}(\text{OH})_4 \cdot \text{H}_2\text{O}$ . *Spectrochimica Acta Part A-Molecular and Biomolecular*  
254 *Spectroscopy*, 91, 314-318.
- 255 Gutzmer, J. and Beukes, N.J. (1996) Mineral paragenesis of the Kalahari manganese  
256 field, South Africa. *Ore Geology Reviews*, 11, 405-428.
- 257 Horiuchi, H., Saito, A., Tachi, T., and Nagasawa, H. (1997) Structure of synthetic  
258  $\text{Li}_2(\text{Mg,Cu})\text{Cu}_2(\text{Si}_2\text{O}_6)_2$ : A unique chain silicate. *American Mineralogist*, 82, 143-  
259 148.
- 260 Kawahara, A. (1976) The crystal structure of shattuckite. *Mineralogical Journal*, 8, 193-  
261 199.
- 262 Kawamura, K., and Kawahara, A. (1976) The crystal structure of synthetic copper  
263 sodium silicate  $\text{Cu}_3\text{Na}_2(\text{Si}_4\text{O}_{12})$ . *Acta Crystallographica*, B32, 2419-2422.
- 264 ----- (1977) The crystal structure of synthetic copper sodium silicate  $\text{CuNa}_2(\text{Si}_4\text{O}_{10})$ .  
265 *Acta Crystallographica*, B33, 1071-1075.
- 266 Kawamura, K., Kawahara, A., and Henmi, K. (1976) Hydrothermal synthesis and X-ray  
267 study of copper silicate hydrate minerals. *Kobutsugaku Zasshi (Journal of*  
268 *Mineralogical Society of Japan)*, 12, 403-414.
- 269 Kleyenstuber, A.S.E. (1984) The mineralogy of the manganese-bearing Hotazel  
270 Formation of the Proterozoic Transvaal sequence of Griqualand West, South

- 271 Africa. *Trans. Geol. Soc. South Africa*, 87, 267-275.
- 272 Libowitzky, E. (1999) Correlation of O-H stretching frequencies and O-H...O hydrogen  
273 bond lengths in minerals. *Monatshefte für Chemie*, 130, 1047-1059.
- 274 Makreski, P., Jovanovski, G., Kaitner, B., Gajovic, A., and Biljan, T. (2007) Minerals  
275 from Macedonia XVII. Vibrational spectra of some sorosilicates. *Vibrational*  
276 *Spectroscopy*, 44, 162-170.
- 277
- 278 Moore, P.B, Davis, A.M, Van Derveer, D.G, Sen Gupta, P.K (1993) Joesmithite, a  
279 plumbous amphibole revisited and comments on bond valences. *Mineralogy and*  
280 *Petrology* 48, 97-113.
- 281 Rinaudo C, Belluso E, Gastaldi D (2004) Assessment of the use of Raman spectroscopy  
282 for the determination of amphibole asbestos. *Mineralogical Magazine*, 68, 455-  
283 465
- 284 Robinson, K., Gibbs, G.V., and Ribbe, P.H. (1971) Quadratic elongation, a quantitative  
285 measure of distortion in coordination polyhedra. *Science*, 172, 567–570.
- 286 Sheldrick, G. M. (2008) A short history of *SHELX*. *Acta Crystallographica*, A64, 112-  
287 122.
- 288 Von Bezing, K.L., Dixon, R.D., Pohl, D., and Cavallo, G. (1991) The Kalahari  
289 Manganese Field, an update. *Mineralogical Record*, 22, 279-297.
- 290 Yang, H., Evans, S.H., Downs, R.T., Jenkins, R.A. (2011) The crystal structure of  
291 vladimirite, with a revised chemical formula,  $\text{Ca}_4(\text{AsO}_4)_2(\text{AsO}_3\text{OH})\cdot 4\text{H}_2\text{O}$ .  
292 *Canadian Mineralogist*, 49, 1055-1064.
- 293 Zöller, M.H., Tillmanns, E., and Hentschel, G. (1992) Liebauite,  $\text{Ca}_3\text{Cu}_5\text{Si}_9\text{O}_{20}$ : A new  
294 silicate mineral with 14er single chain. *Zeitschrift für Kristallographie*, 200, 115-  
295 126.
- 296
- 297
- 298

299 **List of Tables**

300

301 Table 1. Powder X-ray diffraction data for lavinskyite.

302

303 Table 2. Summary of crystallographic data and refinement results for lavinskyite.

304

305 Table 3. Coordinates and displacement parameters of atoms in lavinskyite.

306

307 Table 4. Selected bond distances (Å) in lavinskyite.

308

309 Table 5. Mineralogical data for lavinskyite and planchéite.

310

311 Table 6. Tentative assignment of major Raman bands for lavinskyite.

312

313

314

315

316

317 **List of Figure Captions**

318

319 Figure 1. (a) Rock samples on which lavinskyite crystals are found; (b) A microscopic  
320 view of lavinskyite, associated with dark blue scottyite.

321

322 Figure 2. A backscattered electron image, showing the assemblage of scottyite (light  
323 gray), wesselsite (medium gray), and lavinskyite (dark gray).

324

325 Figure 3. Crystal structure of lavinskyite.

326

327 Figure 4. Crystal structure of lavinskyite. The aquamarine, yellow, green, and blue  
328 spheres represent K, Cu(M4), Li(M4), and H atoms, respectively.

329

330 Figure 5. Raman spectrum of lavinskyite.

331

332

333

334

335

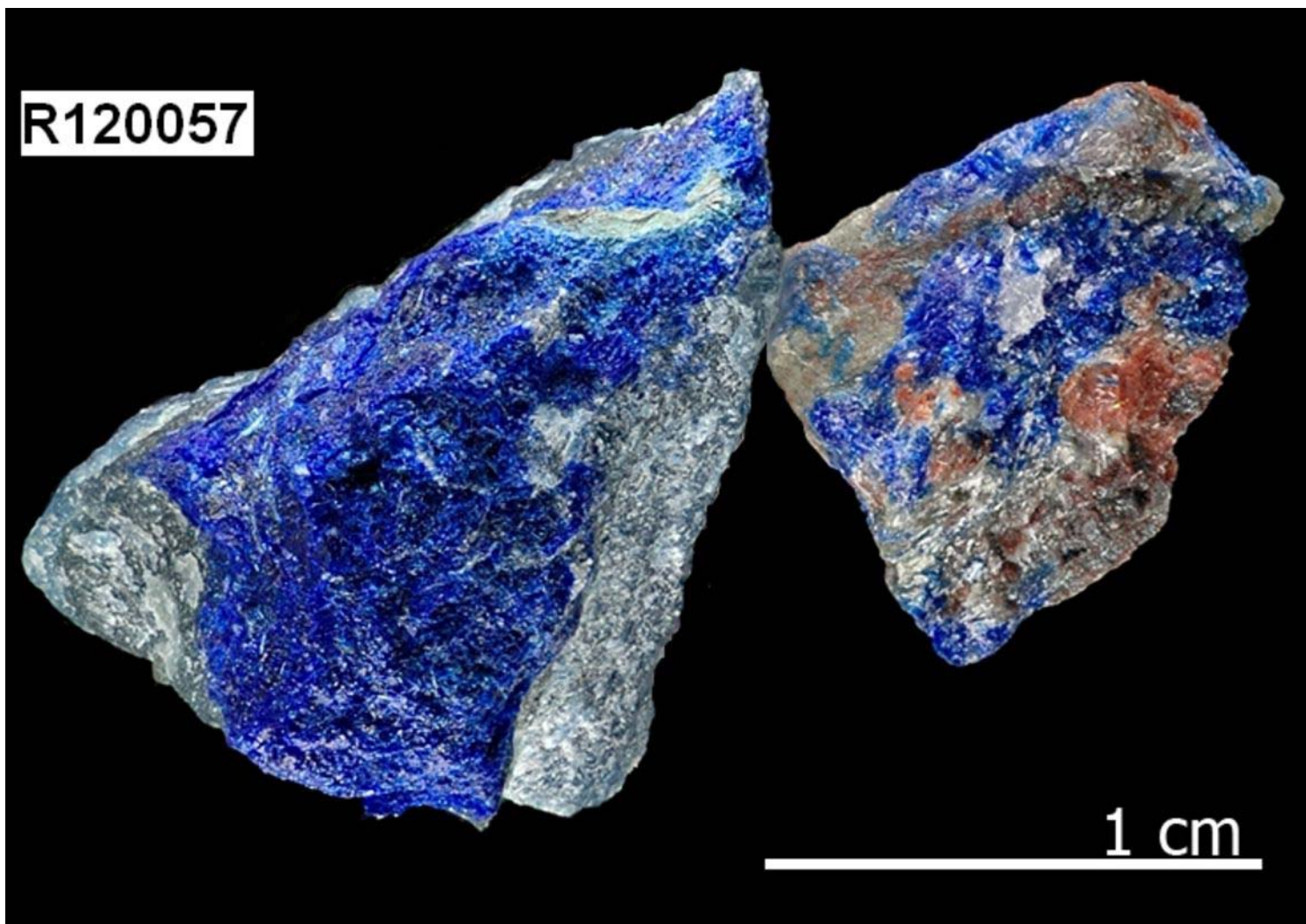
336

337

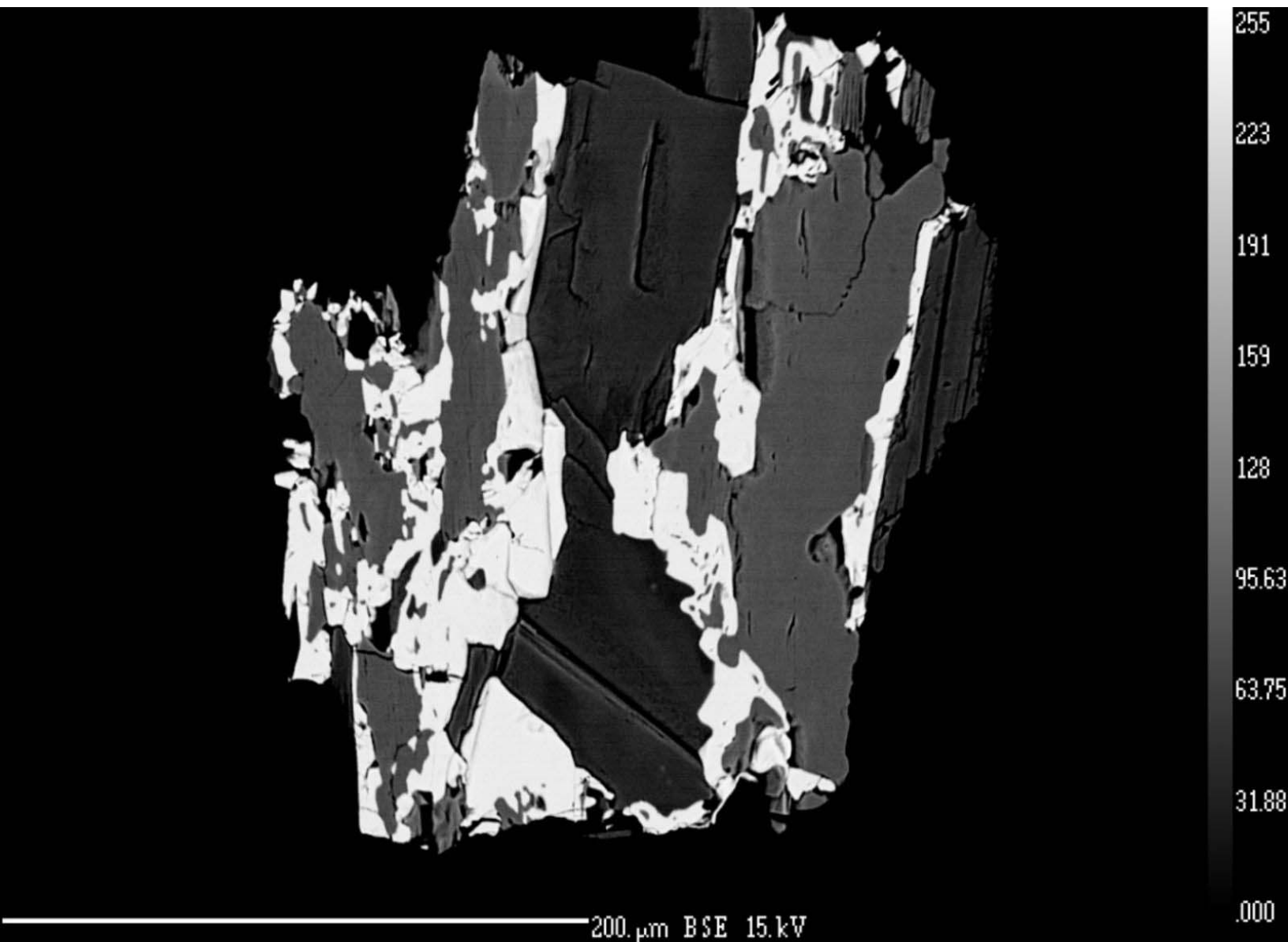
338

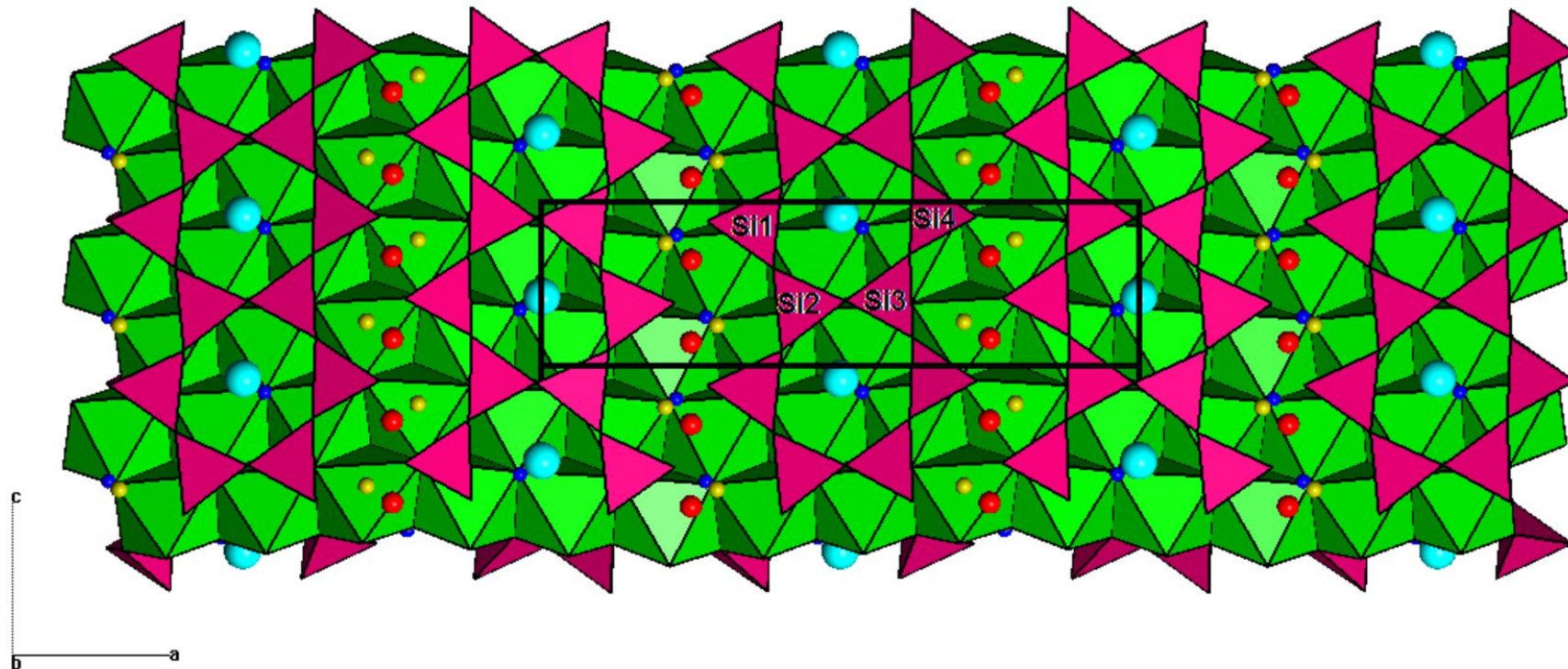
339

340

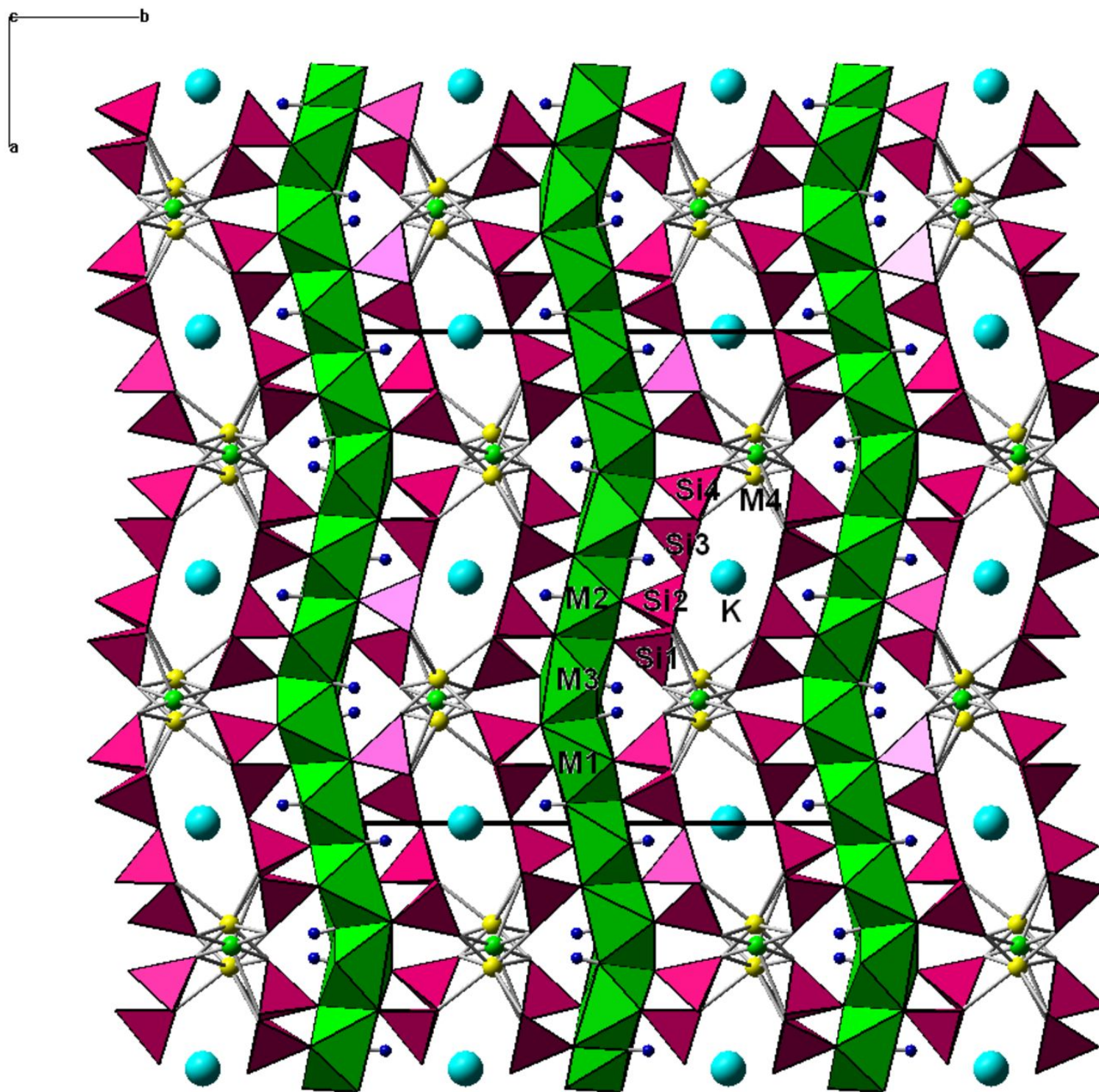












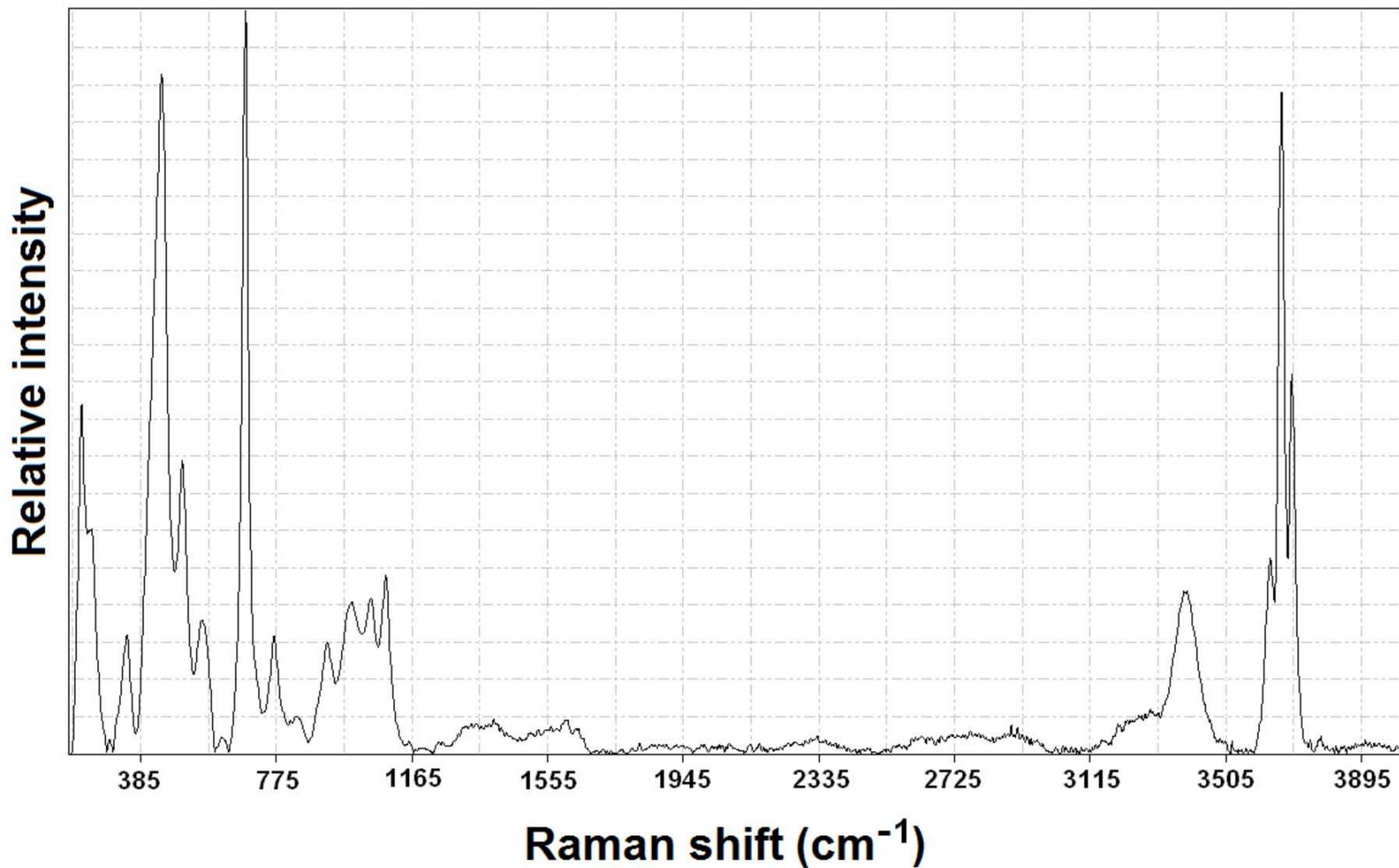


Table 1. Powder diffraction data for strong peaks of lavinskyite

Experimental		Theoretical		
<i>I</i>	<i>d</i> (Å)	<i>I</i>	<i>d</i> (Å)	h k l
100	10.291	100	10.189	0 2 0
13	9.608	9	9.523	2 0 0
8	9.006	16	8.984	1 2 0
18	6.994	5	6.957	2 2 0
18	4.984	24	4.921	1 4 0
6	4.057	11	4.046	3 0 1
11	3.964	19	3.973	3 4 0
2	3.578	11	3.590	1 4 1
27	3.321	30	3.343	1 6 0
6	2.979	9	2.995	3 6 0
3	1.571	11	1.568	12 2 0

Table 2. Summary of crystal data and refinement results for lavinskyite

---

---

Ideal chemical formula	K(LiCu)Cu <sub>6</sub> (Si <sub>4</sub> O <sub>11</sub> ) <sub>2</sub> (OH) <sub>4</sub>
Crystal symmetry	Orthorhombic
Space group	<i>Pcnb</i> (#60)
<i>a</i> (Å)	19.046(2)
<i>b</i> (Å)	20.377(2)
<i>c</i> (Å)	5.2497(6)
<i>V</i> (Å <sup>3</sup> )	2037.4(4)
<i>Z</i>	4
$\rho_{\text{cal}}$ (g/cm <sup>3</sup> )	3.616
$\lambda$ (Å, MoK $\alpha$ )	0.71073
$\mu$ (mm <sup>-1</sup> )	7.403
$2\theta_{\text{max}}$ (°)for data collection	65.36
No. of reflections collected	16336
No. of independent reflections	3702
No. of reflections with $I > 2\sigma(I)$	2639
No. of parameters refined	214
R(int)	0.048
Final $R_1$ , $wR_2$ factors [ $I > 2\sigma(I)$ ]	0.031, 0.057
Final $R_1$ , $wR_2$ factors (all data)	0.058, 0.064
Goodness-of-fit	0.971

---

---

Table 3. Atomic coordinates and displacement parameters for lavinskyite

Atom x	y	z	Uiso	U11	U22	U33	U23	U13	U12
A	0.25	0.9725(2)	0.0239(2)	0.0200(5)	0.0279(6)	0.0238(5)	0	0	-0.0094(5)
M1	0.45964(3)	0.25459(9)	0.0085(2)	0.0092(3)	0.0096(3)	0.0065(3)	0.0029(2)	-0.0024(2)	-0.0029(2)
M2	0.37544(2)	0.77970(7)	0.0096(1)	0.0094(2)	0.0117(2)	0.0077(2)	0.0030(1)	-0.0018(1)	-0.0022(1)
M3	0.29265(2)	0.29637(6)	0.0092(1)	0.0095(2)	0.0122(2)	0.0058(2)	0.0027(1)	-0.0019(1)	-0.0034(1)
M4a	0.25019(3)	0.7061(1)	0.0145(2)	0.0116(3)	0.0074(3)	0.0244(4)	0.0003(2)	-0.0074(3)	0.0001(2)
M4b	0.208(2)	0.814(7)	0.061(7)						
Si1	0.64168(4)	0.10879(4)	0.0066(2)	0.008(4)	0.0068(4)	0.0052(3)	0.0001(3)	-0.0007(3)	-0.0009(3)
Si2	0.56233(4)	0.12204(4)	0.0066(2)	0.008(4)	0.0068(4)	0.0050(3)	0.0002(3)	0.0000(3)	-0.0004(3)
Si3	0.40602(4)	0.15778(4)	0.0065(2)	0.007(3)	0.0075(4)	0.0052(3)	0.0004(3)	0.0003(3)	-0.0011(3)
Si4	0.32834(4)	0.18205(4)	0.0070(2)	0.009(4)	0.0075(4)	0.0048(3)	0.0002(3)	-0.0002(3)	-0.0008(3)
O1	0.6279(1)	0.0311(1)	0.0088(4)	0.0103(10)	0.0074(10)	0.0087(9)	-0.0001(8)	-0.0010(8)	-0.0016(8)
O2	0.5459(1)	0.0455(1)	0.0095(4)	0.0128(11)	0.0080(11)	0.0076(9)	0.0016(8)	0.0003(8)	-0.0020(8)
O3	0.3809(1)	0.0825(1)	0.0086(4)	0.0108(10)	0.0078(10)	0.0071(9)	-0.0002(7)	-0.0017(8)	-0.0033(8)
O4	0.2997(1)	0.1082(1)	0.0116(4)	0.0145(11)	0.0117(11)	0.0087(9)	0.0023(8)	-0.0022(8)	-0.0022(8)
O5	0.7237(1)	0.1273(1)	0.0127(4)	0.0081(10)	0.0149(12)	0.0148(10)	0.0000(8)	-0.0022(8)	-0.0035(8)
O6	0.5984(1)	0.1442(1)	0.0111(4)	0.0156(11)	0.0089(11)	0.0086(9)	0.0001(8)	0.0040(8)	0.0006(8)
O7	0.6125(1)	0.1432(1)	0.0115(4)	0.0161(12)	0.0104(11)	0.0081(9)	0.0007(8)	-0.0041(8)	-0.0022(8)
O8	0.4913(1)	0.1659(1)	0.0122(4)	0.0070(10)	0.0088(11)	0.0206(11)	-0.0007(8)	0.0018(8)	-0.0009(8)
O9	0.3834(1)	0.1913(1)	0.0110(4)	0.0147(11)	0.0111(11)	0.0069(9)	-0.0016(8)	0.0044(8)	-0.0027(8)
O10	0.3782(1)	0.1982(1)	0.0108(4)	0.0170(11)	0.0085(11)	0.0068(9)	0.0013(8)	-0.0032(8)	-0.0031(9)
O11	0.2709(1)	0.2388(1)	0.0161(5)	0.0151(11)	0.0172(13)	0.0160(11)	-0.0019(9)	-0.0028(9)	0.0059(9)
O12	0.4609(1)	0.0603(1)	0.0127(5)	0.0141(11)	0.0108(11)	0.0134(10)	0.0025(9)	-0.0033(9)	-0.0049(9)
O13	0.2851(1)	0.0020(1)	0.0082(4)	0.0084(10)	0.0096(11)	0.0069(9)	0.0014(8)	-0.0002(7)	-0.0011(8)
H1	0.274(3)	0.593(9)	0.04						
H2	0.469(3)	0.916(9)	0.04						

Note: The site occupancies are A = K, M1 = (0.775Cu + 0.225Mg), M2 = Cu, M3 = Cu, M4a = 0.5Cu, M4b = 0.5Li.

Table 4. Selected bond distances in lavinskyite and planchéite.

	lavinskyite	planchéite
	Distance (Å)	Distance (Å)
Si1-O1	1.606(2)	1.608
-O5	1.613(2)	1.629
-O7	1.640(2)	1.646
-O6	1.648(2)	1.637
Ave.	1.630	1.630
TAV*	7.93	
TQE*	1.002	
Si2-O2	1.592(2)	1.635
-O7	1.624(2)	1.704
-O6	1.628(2)	1.530
-O8	1.629(2)	1.612
Ave.	1.630	1.620
TAV	7.98	
TQE	1.002	
Si3-O3	1.607(2)	1.617
-O10	1.615(2)	1.626
-O9	1.617(2)	1.580
-O8	1.635(2)	1.636
Ave.	1.618	1.615
TAV	15.80	
TQE	1.004	
Si4-O11	1.596(2)	1.649
-O4	1.603(2)	1.637
-O10	1.647(2)	1.659
-O9	1.652(2)	1.585
Ave.	1.624	1.633
TAV	22.77	
TQE	1.005	
M1-O2	1.961(2)	1.690
-OH12	1.966(2)	1.844
-O2	2.047(2)	2.158
-O1	2.050(2)	2.155
-OH12	2.287(2)	2.467
-O3	2.422(2)	2.469
Ave.	2.122	2.130

M2-OH12	1.960(2)	2.029
-O1	1.979(2)	1.867
-OH13	1.985(2)	2.079
-O3	2.000(2)	1.869
-O2	2.383(2)	2.687
-O4	2.473(2)	2.279
Ave.	2.130	2.135
M3-O4	1.944(2)	2.220
-OH13	1.982(2)	1.736
-O3	2.000(2)	2.063
-OH13	2.023(2)	2.215
-O4	2.353(2)	2.242
-O1	2.535(2)	2.641
Ave.	2.140	2.186
M4a-O11	1.902(2)	1.945
-O11	1.927(2)	1.798
-O5	1.975(2)	1.839
-O5	1.983(2)	2.022
Ave.	1.947	1.901
M4b-O11	1.907(2)	
-O5	2.091(2)	
-O11	2.286(2)	
-O5	2.399(2)	
-O6	2.494(2)	
-O10	2.699(2)	
Ave.	2.313	
A -O9 x2	2.797(2)	
-O10 x2	2.886(2)	
-O6 x2	3.027(2)	
-O8 x2	3.091(2)	
-O8 x2	3.197(2)	
Ave.	2.998	

---

Note: According to Evans and Mrose (1977), “The bond lengths in planchéite are poorly determined ( $\sigma > 0.1 \text{ \AA}$ ) and are not amenable to detailed interpretation”.

\*: TAV—tetrahedral angle variance; TQE—tetrahedral quadratic elongation (Robinson et al. 1971).

Table 5. Mineralogical data for lavinskyite and planchéite.

	Lavinskyite	Planchéite
Chemical formula	$K(\text{LiCu})\text{Cu}_6(\text{Si}_4\text{O}_{11})_2(\text{OH})_4$	$\text{Cu}_8(\text{Si}_4\text{O}_{11})_2(\text{OH})_4 \cdot \text{H}_2\text{O}$
a(Å)	19.046(2)	19.043(3)
b(Å)	20.377(2)	20.129(5)
c(Å)	5.2497(6)	5.269(1)
V(Å <sup>3</sup> )	2037.4(4)	2019.5(5)
Space group	<i>Pcnb</i> (#60)	<i>Pcnb</i> (#60)
Z	4	4
$\rho_{\text{cal}}(\text{g}/\text{cm}^3)$	3.62	3.82
Strong powder lines	10.188(100) 3.343(32) 2.693(29) 2.522(27) 4.921(25) 2.316(22) 3.973(19)	10.064(100) 4.865(53) 2.694(47) 6.917(43) 3.943(31) 2.520(31) 3.304(27)
$n_\alpha$	1.675	1.697
$n_\beta$	1.686	1.718
$n_\gamma$	1.715	1.741
2V(°)	64(+)	88.5(+)
Reference	(1)	(2)

(1) This work; (2) Evans and Mrose (1977).



Table 6. Tentative assignments of major Raman bands for lavinskyite

Bands (cm <sup>-1</sup> )	Intensity	Assignment
3694, 3662, 3630 3390	Weak to Strong, sharp	O-H stretching vibrations
1090, 1043, 991 919, 891	Relatively weak and broad	Si-O symmetric and anti-symmetric stretching modes within SiO <sub>4</sub> tetrahedra
685	Strong, sharp	Si-O-Si bending
580, 562, 503, 445 424, 401	Relatively strong	O-Si-O symmetric and anti-symmetric bending modes within SiO <sub>4</sub> tetrahedra
<400	Strong to weak	SiO <sub>4</sub> rotational modes, lattice vibrational modes, and Cu-O interactions